Turkish Journal of Chemistry

http://journals.tubitak.gov.tr/chem/

Research Article

Turk J Chem
(2017) 41: 944 – 954

doi:10.3906/kim-1701-34

A promising materials approach to combatting renal hyperphosphatemia: Fe(II)-montmorillonites

Xiaotong YUAN[1], Dawei QIN[1,*], Min QIAO[2], Gang LIU[2], Hongxin LI[2], Xia NIU[1]
[1]Qilu University of Technology, Jinan, Shandong, P.R. China
[2]Shandong SiBang Pharmaceutical Co., Ltd, Jinan, Shandong, P.R. China

Received: 14.01.2017 • **Accepted/Published Online:** 21.06.2017 • **Final Version:** 20.12.2017

Abstract: The objective of the current effort was to determine the efficacy of Fe(II)-montmorillonite (Fe(II)-MMT) as an adjuvant for specific targeted adsorption of phosphate. Specifically, Fe(II)-MMT was studied to combat hyperphosphatemia and anemia arising from chronic renal failure. The adsorption of phosphate over time, pH, and initial concentration was studied. The systems were characterized by X-ray diffraction (XRD), Raman, and zeta potential. The experimental results demonstrated the adsorption time was set to 140 min to achieve maximum adsorption efficiency. It was thus found that the maximum adsorption was at pH 3.0. In addition, it reached equilibrium when the initial phosphate concentration was at 60 mg/L while the maximum adsorption capacity was 5.75 mg of phosphate/g of Fe(II)-MMT. On the other hand, adsorption isotherms showed that the Langmuir model was better than the Freundlich model. This means that the adsorption of the phosphate on Fe(II)-montmorillonites was monolayer adsorption, and the phosphate was successfully adsorbed either onto the surface or intercalated within interlayer volume. Live experiments supported the ability of Fe (II)-MMT to control hyperphosphatemia and treat chronic renal failure.

Key words: Adsorption, phosphate, Fe(II)-montmorillonites, chronic renal failure, hyperphosphatemia

1. Introduction

Hyperphosphatemia is a precursor to secondary hyperparathyroidism[1–3] and soft tissue and vascular calcification in chronic kidney disease (CKD), which increases the independent risk factors of chronic kidney disease patients in the incidence of cardiovascular diseases, morbidity, mortality, and hospitalization rates.[4–6] Meta-analysis has shown that the risk for mortality and cardiovascular death increased 18% and 10%,[7] respectively, when blood phosphorus increased by 0.323 mmol/L CKD. Hyperphosphatemia causes vascular calcification and increases the incidence of reactive oxygen species that obstruction proper endothelial function. In addition, hyperphosphatemia increases parathyroid hormone (PTH) and fibroblast growth factor- 23 (FGF-23) and inhibits the synthesis of dihydroxy vitamin D3, leading to cardiac vascular disease (CVD) complications.

NKF-K/DOQI guidelines recommend a target for blood phosphorus in CKD patients after dialysis of 1.13–1.78 mmol/L, but clinical success rates are not promising.[8,9] DOPPS studies have shown that the prevalence of hyperphosphatemia in hemodialysis patients was 57.4% and the prevalence of hyperphosphatemia in peritoneal dialysis patients was 47.7%, while the success rate of blood phosphorus control was only 38.5%.[10] The

*Correspondence: daweiqin109@163.com

main treatment for hyperphosphatemia was food intake control[11,12] and reduction of the intestinal absorption of phosphorus and blood dialysis using a phosphate binder. Excessive diet, however, leads to insufficient protein intake, while regular dialysis treatment for phosphorus removal is limited. Therefore, more than 90% of dialysis patients must control their blood phosphorus[13] by oral phosphate binders. Intestinal phosphorus binders include calcium, aluminum phosphate, sevelamer hydrochloride,[14] and lanthanum carbonate.[15−17] Aluminum can lead to erythropoietin anemia, bone disease, and adverse reactions. Calcium phosphate causes hypercalcemia and increases the risk of metastatic calcification, thus limiting this clinical application. Sevelamer hydrochloride and lanthanum carbonate reduce blood phosphorus without causing blood calcium increases.[18−20] However, an exorbitant price limits its widespread appeal. Ferric iron compounds SBR759 in preliminary period clinical trials demonstrated effective reduction of the CKD5 period in patients with maintenance hemodialysis blood phosphorus levels. The comparison of a potentially random curative effect between SBR759 and sevelamer hydrochloride was conducted between hemodialysis patients[21] in Asia for 12 weeks showing a therapeutic effect within the SBR759 group better than of the sevelamer hydrochloride group; both calcium concentrations were unchanged, adverse reactions and the incidence of serious adverse events were similar, but the overall drug withdrawal rate of the SBR759 group was lower than that of the sevelamer hydrochloride group.

In addition, chronic renal failure patients have inadequate intake or excessive loss of iron. Moreover, an absolute or relative deficiency in erythropoietin (EPO) can cause renal anemia.[22,23] Anemia can lead to heightened incidences of cardiovascular[24−26] events in patients with CKD and reduce their quality of life. DOPPS studies suggested that in cases where hemoglobin was administered to patients receiving hemodialysis (hemoglobin, Hb), the mortality and hospitalization rates decreased 10% and 12%, respectively. In recent years, phosphate binders containing iron, such as SBR759 and PA21- 1, have entered clinical trials with distinct curative effects.[27,28]

Recently, much effort has been devoted to applications of montmorillonite (MMT) in biological fields, especially drug delivery systems.[29−31] According to the previous reports, MMT is a biocompatible material. We tested the effects of Fe(II)-montmorillonite on adenine-induced chronic renal failure in rats with hyperphosphatemia[32] and obtained satisfactory results. In addition, since MMT is a common ingredient in pharmaceutical products, it is also capable of blood compatibility.[33,34] Fe(II)-montmorillonites are a new type of biocompatible phosphate binder that are able to dissociate free iron and montmorillonite in vivo. Iron bonding with phosphate forms insoluble substances that are excreted, while dissociated montmorillonite is not absorbed and thus can be tuned to achieve a therapeutic aim for high phosphorus. Simultaneously, any excess iron from the montmorillonite solution that did not combine with phosphate can be absorbed to supplement the iron losses found in chronic renal failure patients.

The present study studied the adsorption of phosphate by Fe(II)-MMT under different adsorption conditions including time, pH, and initial phosphate concentration. It should be noted that the concentration of the Fe(II) measured by UV-vis spectrophotometer under all experimental condition was 80 mg/L after several measurements.[32] A possible binding phenomenological construct of MMT that includes Fe(II) and phosphate is presented in Figure 1. Live experiments were carried out by detecting P (mol L^{-1}), red blood cells (RBC), Hb, red blood cell specific volume (HCT), EPO, single positive (SP), and albumin (ALB) in male golden hamsters.

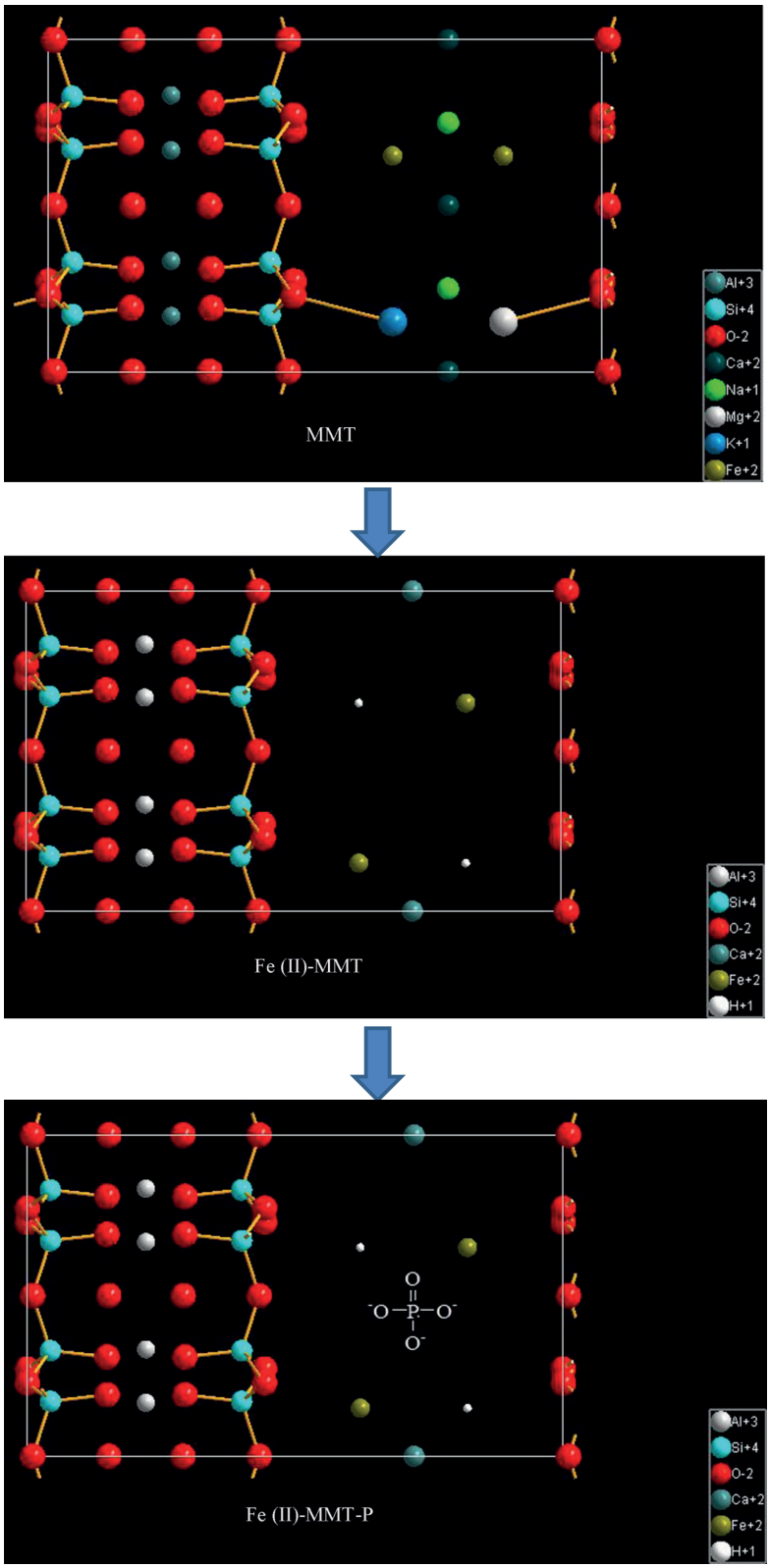

Figure 1. Possible structural arrangement of MMT and adsorption of Fe(II) and phosphate.

2. Results and discussion

2.1. Effect of time on the adsorption of phosphate

The experiments were carried out to optimize the time required for maximum adsorption of phosphate onto Fe(II)-MMT. Figure 2 shows the effect of time on the adsorption of phosphate. The adsorption rate (the slope) of phosphate was high within 90 min, indicating that the adsorption greatly increased. At 140 min, the adsorption no longer increased, indicating that the equilibrium adsorption was being approached. Therefore, the adsorption time was set to 140 min to achieve maximum adsorption efficiency.

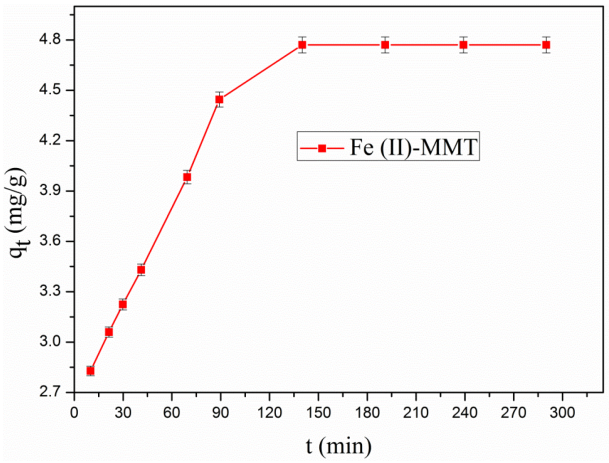

Figure 2. The effect of time on the adsorption of phosphate onto Fe(II)-montmorillonites (adsorption conditions: initial condition = 40 mg/L, temperature = 298 K, pH = 2.0).

The capacity of phosphate adsorption at equilibrium was calculated from the following equation:

$$q_e = \frac{(C_0 - C_e)\,V}{m} \tag{1}$$

where q_e (mg/g) is the phosphate species adsorbed at equilibrium, C_0 (mg/L) is the initial solution concentration of phosphate, C_e (mg/L) is the equilibrium concentration of phosphate in solution, V (L) is the volume of aqueous solutions containing phosphate, and m (g) is the mass of Fe(II)-montmorillonites.

2.2. Effect of pH on the adsorption of phosphate

To determine the effect of pH on adsorption capacity, pH levels ranging from 1 to 10 were prepared. Phosphate and Fe(II)-MMT systems were treated at different pH at constant temperature (37 °C), time (140 min), and concentration (40 mg/g). As shown in Figure 3, the adsorption capacities were similar except for at pH 3.0, at which it was 3.7 mg/g. Fe(II)-MMT can allow Fe(II) and MMT to leach, while the leached Fe(II) can combine with phosphate to form an insoluble precipitate and serve to remove phosphate. With an increase in pH, Fe(II) can be oxidized and cannot combine with phosphate; thus, the adsorption capacity decreased. The pH value should be appropriate in the human body. The pH value is too high or too low, which are not conducive to the release of Fe(II) ion. It is known that Fe(II) ion would be hydrolyzed at pH $<$ 2.0; on the other hand, Fe(II) ion may be complexed at pH $>$ 10. It was thus found that the maximum adsorption was at pH 3.0.

2.3. Effect of initial phosphate concentration on its adsorption onto Fe(II)-MMT

To achieve maximum adsorption, the experiments were performed at different initial concentrations of phosphate at constant temperature (37 °C), time (140 min), and pH (3.0). As shown in Figure 4, as the initial concentration of phosphate in the solution increased, the amount of adsorption increased, a phenomenon ascribed to a greater concentration gradient at the onset. However, it reached equilibrium when the initial phosphate concentration was at 60 mg/L while the maximum adsorption capacity was 5.75 mg of phosphate/g of Fe(II)-MMT.

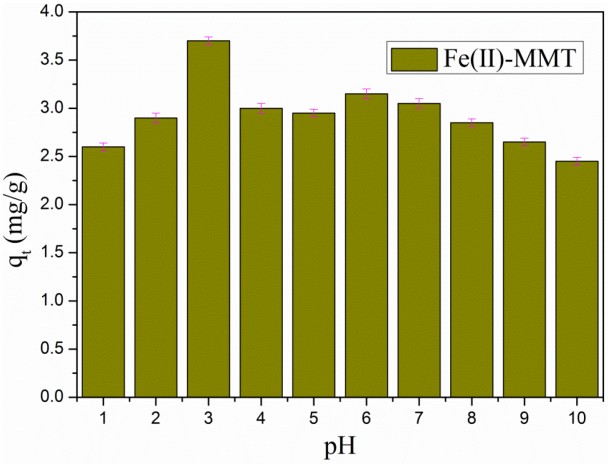

Figure 3. Effect of pH value on the adsorption of Fe(II)-montmorillonites for phosphate (adsorption conditions: initial condition = 40 mg/L, adsorption time = 140 min, temperature = 310 K).

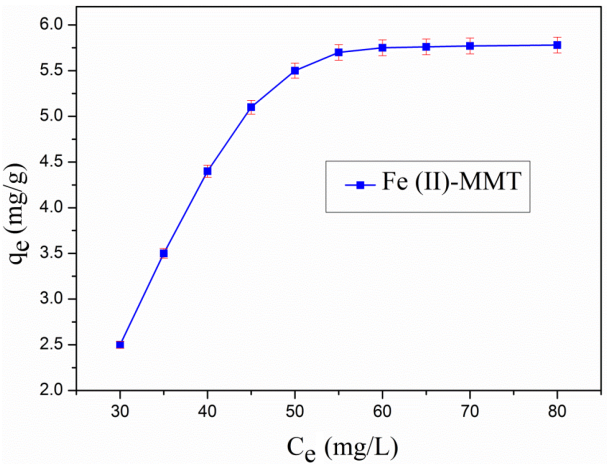

Figure 4. Effect of initial concentration on the adsorption of Fe(II)-montmorillonites for phosphate (adsorption conditions: pH = 3.0, adsorption time = 140 min, and temperature = 310 K).

2.4. Analyses of adsorption isotherms

The experiments were carried out to determine the adsorbent concentration of phosphate onto Fe(II)-MMT. Figure 5 showed the fitting plots of Langmuir[35] (a) and Freundlich[36] (b) adsorption isotherms of the phosphate on Fe(II)-montmorillonites at 310 K (plots at 303 K and 308 K were not shown), respectively. The Langmuir isotherm Eq. (2) was given by

$$\frac{1}{q_e}=\frac{1}{q_m}+\frac{1}{q_m bC_e} \tag{2}$$

where q_e (mg/g) is the amount adsorbed at equilibrium, q_m (mg/g) is the maximum monolayer adsorption capacity, C_e (mg/L) is the equilibrium concentration of the phosphate buffer solution, and b (L/mg) related to the free energy of adsorption, respectively. Plots of $1/q_e$ versus $1/C_e$ values can be used to determine q_m and b.

The Freundlich isotherm Eq. (3) is an empirical equation given by

$$\ln q_e=\ln K_F+\frac{1}{n}\ln C_e, \tag{3}$$

where q_e (mg/g) is the amount adsorbed at equilibrium, K_F [mg/g(L/mg)1/n] and n is the empirical parameter related to the adsorption capacity and intensity adsorption, and C_e (mg/L) is the equilibrium concentration of the phosphate buffer solution. The linear plot of $\ln q_e$ versus $\ln C_e$ can give K_F and n.

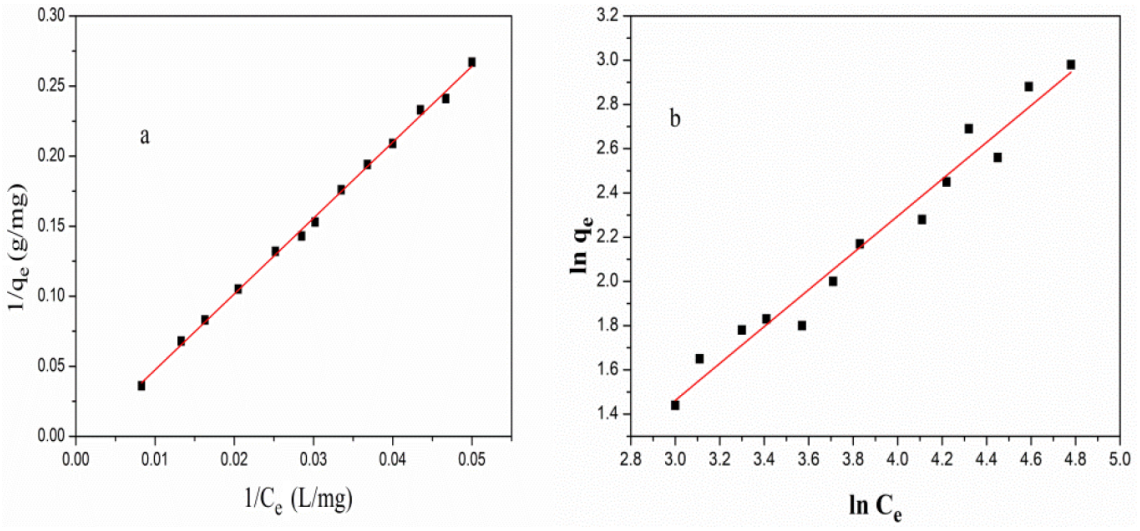

Figure 5. The Langmuir (a) and Freundlich (b) isotherms linear models for the adsorption of Fe(II)-montmorillonites for the phosphate (adsorption conditions: pH = 3.0, adsorption time = 140 min, and temperature = 310 K).

The fitted constants of the Langmuir and Freundlich models are shown in Table 1.

Table 1. Adsorption isotherms parameters of the phosphate onto Fe(II)-montmorillonites at different temperatures.

Temperature (K)	Langmuir isotherm			Freundlich isotherm		
	q_m(mg g^{-1})	K_L (L g^{-1})	R^2	K_F (mg g^{-1})	R^2	$1/n$
303	13.5	0.0132	0.9982	0.4359	0.9276	1.2746
308	15.1	0.0119	0.9985	0.3968	0.9589	1.2456
310	16.8	0.0110	0.9989	0.3541	0.9671	1.1998

R^2 in the table represented the regression coefficient. It clear that the experimental data fitted the Langmuir models well ($R^2 > 0.998$); this means that the adsorption of the phosphate on Fe(II)-montmorillonites was monolayer adsorption.

2.5. X-ray diffraction analysis

XRD patterns of Fe(II)-MMT and Fe(II)-MMT with adsorbed phosphate are illustrated in Figure 6. The characteristic 2θ peak of the (001) plane for Fe(II)-MMT and Fe(II)-MMT adsorption of phosphate hybrid is at 6.11° and 6.38°, with basal spacing (d_{001}) of 15.1 Å and 14.4 Å, respectively. According to Bragg's equation, the diffraction peak shifting from higher angle to lower angle is due to the increase in d_{001} spacing, which indicates that at least part of phosphate has been effectively intercalated into the interlayer of Fe(II)-MMT during the adsorption process.[37]

2.6. Raman spectroscopy analysis

Raman spectroscopy can be used to analyze chemical and structural changes at the micrometer scale level (1 μm) on the surface.[37] As shown in Figure 7, the band at 306 cm^{-1} is caused by the bending vibration modes of Mg–O bonds. The band at 347 cm^{-1} is related to the shift of 326 cm^{-1} bending vibration modes, which corresponds to the Fe–O bonds. The Raman bands at 588 cm^{-1} and 638 cm^{-1} are attributed to the vibrational

modes of Si–O–Si bonds, which comprise the SiO_4 tetrahedra that make up a layer.[38] The band at 856 cm^{-1} is due to the stretching vibration of the Si–O bond in SiO_4 tetrahedra. The band at 1074 cm^{-1} may be related to the PO_2 stretching vibration band.[39] In addition, a new band emerged at 940 cm^{-1}, which corresponded to the P–$(OH)_2$ stretching bonds in phosphate aqueous solution,[39] suggesting the presence of phosphorus after adsorption.

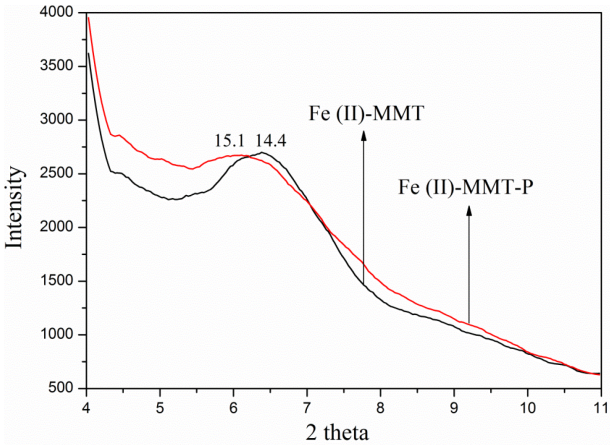

Figure 6. XRD patterns of Fe(II)-montmorillonites and Fe(II)-montmorillonites with adsorbed phosphate.

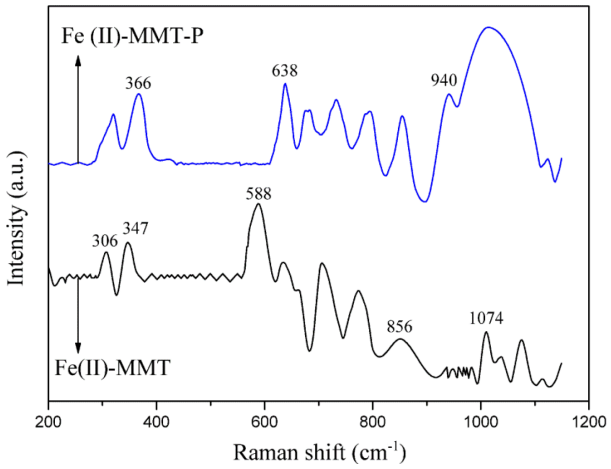

Figure 7. Raman spectra of Fe(II)-montmorillonites and Fe(II)-montmorillonites with adsorbed phosphate.

2.7. Zeta potential

Figure 8 shows the zeta potential curves of two studied samples. Fe(II)-MMT and Fe(II)-MMT-P show similar behavior, with persistent negative zeta potentials that become more negative with increasing pH. The zeta potential value of Fe(II)-MMT with adsorbed phosphate is more negative than Fe(II)-MMT, indicating that phosphate contributed to the negative zeta potential,[40] as it was absorbed onto the surface or intercalated into the interlayer spaces of Fe(II)-MMT.

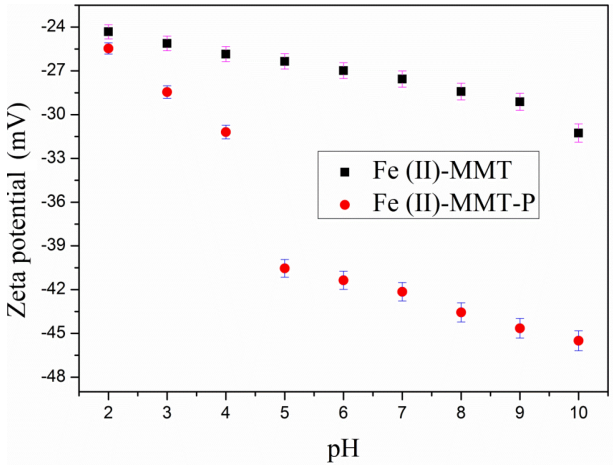

Figure 8. Zeta potential measurements of Fe(II)-montmorillonites and Fe(II)-montmorillonites with adsorbed phosphate.

2.8. Analyses of live experiments

The live experiments had three groups: normal control group (n = 10), adenine-induced chronic renal failure model group (n = 10), and adenine-induced chronic renal failure with added Fe(II)-MMT treatment group (n = 10). The normal control group was gavaged using 2 mL/120 g water daily, the model group was gavaged using 0.5% adenine 2 mL/120 g daily, and the treatment group was gavaged using 0.5% adenine 2 mL/120 g and then 300 mg/kg Fe(II)-montmorillonites after 2 weeks. The above animals were continuously gavaged for 6 weeks, after which blood sampling from the sixth week was done to detect P (mol L^{-1}) RBC (10^{10}), Hb (g/L), HCT (%), EPO (mu/mL), SP (g/L), and ALB (g/L). The results are shown in Tables 2 and 3.

Table 2. The test results of chronic renal failure hyperphosphatemia.

Group	Number (n)	P (mol L^{-1})
Normal control group	10	2.82 ± 0.26
Model control group	10	5.42 ± 0.33
Treatment group	10	3.32 ± 0.24

Table 3. The RBC, Hb, HCT, EPO, SP, and ALB test results of chronic renal failure anemia.

Group	Number (n)	RBC (10^{10})	Hb (g/L)	HCT (%)	EPO (mu/mL)	SP (g/L)	ALB (g/L)
Normal control group	10	6.70 ± 0.54	125.5 ± 7.4	40.7 ± 3.20	9.15 ± 0.67	78.85 ± 1.61	41.85 ± 2.30
Model control group	10	5.20 ± 0.25	90.0 ± 5.7	34.5 ± 1.75	5.70 ± 1.91	65.75 ± 3.78	31.05 ± 1.73
Treatment group	10	6.50 ± 0.52	117.0 ± 7.7	39.7 ± 3.30	7.53 ± 0.57	73.50 ± 1.78	36.30 ± 1.67

Fe(II)-montmorillonites reduce the blood phosphorus of hyperphosphatemia rats, thereby reducing the occurrence of hyperphosphatemia. In Table 3, Fe(II)-montmorillonites show room for improvement in the decline of chronic renal failure anemia model RBC, Hb, and HCT caused by adenine. Meanwhile there is also room for improvement for EPO, SP, and ALB.

3. Experimental

3.1. Materials

Montmorillonites with a cation-exchange capacity (CEC) of 80 mmol/100 g were obtained from Shandong SiBang Pharmaceutical Co., Ltd. The chemical composition of the montmorillonites was determined by X-ray fluorescence spectroscopy: SiO_2 (60.18%), Al_2O_3 (15.79%), Fe_2O_3 (5.38%), MgO (5.20%), H_2O (2.63%), CaO (2.32%), K_2O (0.52%), TiO_2 (0.35%), FeO (0.12%), Na_2O (0.1%), with a loss on ignition of 7.41%. The preparation of Fe(II)-MMT sample has already been described.[32] Thirty healthy male golden hamsters weighing 120 g ± 20 g were provided by the Experimental Animal Center of Shandong University. All chemicals used were analytical reagent grade and obtained from Aladdin Reagent (China). N_2-gas was used for adsorption. All pH in the experiments was measured with a pHS-3C acidity meter.

3.2. Adsorption experiments

The adsorption experiments were conducted to optimize the time required for maximum adsorption of phosphate onto Fe(II)-MMT. First 200 mL of aqueous solution of phosphate containing 13.1 mg of sodium dihydrogen phosphate and 6.6 mg of ascorbic acid were mixed with 100 mg of Fe(II)-MMT powder for 10, 20, 30, 40, 70, 90, 140, 190, 240, and 290 min at 37 °C in a 250-mL conical flask with constant temperature oscillation.

The mixtures were centrifuged and then the concentration of phosphate in the supernatant was determined by UV-vis spectroscopy at λ_{max} = 700 nm. Similarly, the experiments were carried out to determine the optimum pH and maximum adsorption of phosphate onto Fe(II)-MMT at pH of 1, 2, 3, 4, 5, 6, 7, 8, 9, and 10 and the initial amounts were 9.9, 11.5, 13.1, 14.8, 16.4, 18.1, 19.7, 21.4, 23, and 26.3 mg, respectively. All the experimental data were repeated three times and the relative errors ranged within $\pm 3\%$.

3.3. Characterization of materials

The total amounts of phosphate in solutions were determined by T6 UV-vis spectrophotometer (PGENERAL) at 700 nm equipped with a quartz cell having a path length of 1 cm. X-ray diffraction (XRD) patterns were obtained on a Bruker D8 Advance diffraction analyzer, using Cu Kα radiation. XRD data was obtained in the 2 θ range from 3° to 10°. Raman spectra were recorded on a NEXUS 670 spectrograph at a resolution = 0.09 cm^{-1} and laser wavelength = 633 nm. The zeta potential measurements were carried out using the JS94H micro electrophoresis apparatus. Fe(II)-MMT and Fe(II)-MMT-P suspensions (0.5 g L^{-1}) were prepared by dispersing the samples (0.05 g) in distilled water (100 mL). pH of the suspension was raised to $\sim$2 with HCl and the zeta potential measurement was carried out. The pH was slightly increased with NaOH and a new measurement was performed.[41] This procedure was continued until the pH was around 10.0.

3.4. Live experiments

The treatment with Fe(II)-montmorillonites for chronic renal failure hyperphosphatemia is as follows:

Thirty male golden hamsters weighing 120 g $\pm$ 20 g were randomized into 3 groups with 10 per group.

(1) Normal control group: After fully nourishing the mice for 2 weeks and using 2 mL/120 g water to gavage daily.

(2) Model control group: gavage using 0.5% adenine 2 mL/120 g daily.

(3) Treatment group: gavage using 0.5% adenine 2 mL/120 g, then gavage with 300 mg/kg Fe(II)-montmorillonites after 2 weeks.

The above animals were continuously gavaged for 6 weeks, after which blood sampling was done from the sixth week to detect P (mol L^{-1}).

The treatment with Fe(II)-montmorillonites for anemia caused by chronic renal failure is as follows:

Thirty healthy male golden hamsters weighing 120 g $\pm$ 20 g were randomized into 3 groups with 10 in each.

(1) Normal control group: After fully nourishing the mice over 2 weeks, 2 mL/120 g water was used to gavage daily.

(2) Model control group: gavage using 0.5% adenine 2 mL/120 g daily.

(3) Treatment group: gavage using 0.5% adenine 2 mL/120 g, then gavage with 300 mg/kg Fe(II)-montmorillonites after 2 weeks.

The above animals were continuously gavaged over 6 weeks, after which blood sampling was done from the sixth week to detect RBC, Hb, HCT, EPO, SP, and ALB.

4. Conclusions

The adsorption of phosphate onto Fe(II)-MMT attained equilibrium within 140 min. It was thus found that the maximum adsorption was at pH 3.0. In addition, it reached equilibrium when the initial phosphate concentration was at 60 mg/L while the maximum adsorption capacity was 5.75 mg of phosphate/g of Fe(II)-MMT.

Experimental parameters such as time, pH, and initial concentration were investigated and optimized. The optimum condition of the study is that the maximum amount of phosphate adsorption onto Fe(II)-MMT was 5.75 mg/g within 140 min at pH 3.0 and 37 °C. Adsorption isotherms showed that the Langmuir model was better than the Freundlich model. This means that the adsorption of the phosphate on Fe(II)-montmorillonites was monolayer adsorption, and the phosphate was successfully adsorbed either onto the surface or intercalated within interlayer volume.

XRD of Fe(II)-MMT before and after the adsorption phosphate showed that the basal spacing d_{001} increased from 14.4 Å to 15.1 Å, while Raman spectroscopy showed the presence of phosphorus after adsorption. Increasingly negative zeta potential distributions also confirmed the uptake of phosphate. The live experiments showed that Fe(II)-MMT reduced the content of phosphate effectively, and effectively confirmed the adsorption of phosphate onto Fe(II)-MMT. Otherwise, it demonstrated that Fe(II)-MMT can combat hyperphosphatemia and anemia arising from chronic renal failure. These studies serve to support the notion that Fe(II)-MMT may be a promising drug delivery system for the treatment of chronic renal failure. In the future, more chronic renal failure patients will get timely treatment. There is no doubt that it will play a great role in promoting for the medical profession.

Acknowledgments

The research was supported by Shandong SiBang Pharmaceutical Co. Ltd, which signed an industry–university–research cooperation agreement with us.

References

1. Taddei, S.; Nami, R.; Bruno, R. M.; Quatrini, I.; Nuti, R. *Heart. Fail. Rev.* **2011**, *16*, 615-620.
2. Wojcicki, J. M. *Bmc. Nephrol.* **2013**, *14*, 1-12.
3. Yap, Y. S.; Chi, W. C.; Lin, C. H.; Wu, Y. W.; Liu, Y. C. *Int. Urol. Nepgrol.* **2013**, *45*, 163-172.
4. Fourtounas, C. *Hippokratia* **2011**, *15*, 50-52.
5. Isakova, T.; Gutiérrez, O. M.; Wolf, M. *Kidney International* **2009**, *76*, 705-716.
6. Park, S. H.; Stenvinkel, P.; Lindholm, B. *J. Renal. Nutr.* **2012**, *22*, 120-127.
7. Noordzij, M.; Korevaar, J. C.; Boeschoten, E. W.; Dekker, F. W.; Bos, W. J.; Krediet, R. T. *Am. J. Kindey. Dis.* **2005**, *46*, 925-932.
8. Nadkarni, G. N.; Uribarri, J. *Adv. Nutr.* **2014**, *5*, 98-103.
9. Palmer, S. C.; Hayen, A.; Macaskill, P.; Pellegrini, F.; Craig, J. C.; Elder, G. J.; Strippoli, G. F. *Jama-J. Am. Med. Assoc.* **2011**, *305*, 1119-1127.
10. Molony, D. A.; Stephens, B. W. *Adv. Chronic. Kidney. D.* **2011**, *18*, 120-131.
11. Sinha, A.; Prasad, N. *Clinical Queries Nephrology.* **2014**, *3*, 38-45.
12. Kumar, P. A.; Chitra, P. S.; Reddy, G. B. *Rev. Endocr. Metab. Dis.* **2013**, *14*, 273-286.
13. Joshi, G. V.; Kevadiya, B. D.; Patel, H. A.; Bajaj, H. C.; Jasra, R. V. *Int. J. Pharm.* **2009**, *374*, 53-57.
14. Gulati, A.; Sridhar, V.; Bose, T.; Hari, P.; Bagga, A. *Int. Urol. Nepgrol.* **2010**, *42*, 1055-1062.

15. Zhang, C.; Wen, J.; Li, Z.; Fan, J. *BMC Nephrol.* **2013**, *14*, 226.
16. Gros, B.; Galán, A.; Gonzálezparra, E.; Herrero, J. A.; Echave, M.; Vegter, S.; Tolley, K.; Oyagüez, I. *Health. Econ. Rev.* **2015**, *5*, 1-9.
17. Zhai, C. J.; Yang, X. W.; Sun, J.; Wang, R. *Int. Urol. Nepgrol.* **2015**, *47*, 527-35.
18. Kaul, A.; Mahapatra, A. K. *Clinical Queries Nephrology* **2012**, *1*, 134-137.
19. Biggar, P. H.; Liangos, O.; Fey, H.; Brandenburg, V. M.; Ketteler, M. *Pediatr. Nephrol.* **2011**, *26*, 7-18.
20. Stein, D. R.; Feldman, H. A.; Gordon, C. M. *Pediatr. Nephrol.* **2012**, *27*, 1341-1350.
21. Ali, T. M.; Genina, A. M.; Abo-Salem, O. M. *Beni-Suef Univ. J. Basic Appl. Sci.* **2014**, *3*, 133-139.
22. Fishbane, S. *Semin. Nephrol.* **2006**, *26*, 319-324.
23. Ghobrial, E. E.; Salama, K. M.; Shiba, M. F.; Shafae, N. H. E. *Egyptian Pediatric Association Gazette* **2013**, *61*, 37-41.
24. Levin, A.; Foley, R. N. *Am. J. Kidney Dis.* **2000**, *36*, 24-30.
25. Locatelli, F.; Marcelli, D.; Conte, F.; D'Amico, M.; Del, V. L.; Limido, A.; Malberti, F.; Spotti, D. *Nephrol. Dial. Transpl.* **2000**, *15 Suppl 5*, 69.
26. Wahbi, N.; Dalton, R. N.; Turner, C.; Denton, M.; Abbs, I.; Swaminathan, R. *Int. J. Clin. Exp. Patho.* **2001**, *54*, 470.
27. Wu, Y.; Zhou, N.; Li, W.; Gu, H.; Fan, Y.; Yuan, J. *Mat. Sci. Eng. A-struct.* **2013**, *33*, 752-757.
28. Akelah, A.; Rehab, A.; El-Gamal, M. M. *Mat. Sci. Eng. C-struct.* **2008**, *28*, 1123-1131.
29. Zhou, N.; Fang, S.; Xu, D.; Zhang, J.; Mo, H.; Shen, J. *Appl. Clay. Sci.* **2009**, *46*, 401-403.
30. Ding, X.; Li, L.; Liu, P. S.; Zhang, J.; Zhou, N. L.; Lu, S.; Wei, S. H.; Shen, J. *Polym. Composite.* **2010**, *30*, 976-981.
31. Parida, U. K.; Nayak, A. K.; Binhani, B. K.; Nayak, P. L. *Journal of Biomaterials & Nanobiotechnology* **2011**, *02*, 414-425.
32. Qin, D.; Niu, X.; Qiao, M.; Liu, G.; Li, H.; Meng, Z. *Appl. Surf. Sci.* **2015**, *333*, 170-177.
33. Chen, Y.; Bo, L.; Zhou, A.; Liang, J. *Acta. Mater. Compos. Sin.* **2010**, *6*, 237-260.
34. Wang, L.; Chen, J. W.; Ren, F. M.; Wei-Bing, X. U.; Zhou, Z. F. *China Plastics Industry.* **2012**.
35. Langmuir, I. *J. Am. Chem. Soc.* **1915**, *37*, 208-235.
36. Freundlich, H.; Heller, W. *J. Am. Chem. Soc.* **2002**, *61*, 861-870.
37. Borgnino, L.; Avena, M. J.; Pauli, C. P. D. *Colloid. Surface. A* **2009**, *341*, 46-52.
38. Bishop, J. L.; Murad, E. *J. Raman. Spectrosc.* **2004**, *35*, 480-486.
39. Preston, C. M.; Adams, W. A. *Chemischer Informationsdienst.* **1979**, *10*, 814-821.
40. Borgnino, L.; Giacomelli, C. E.; Avena, M. J.; Pauli, C. P. D. *Colloid. Surface. A* **2010**, *353*, 238-244.
41. Perassi, I.; Borgnino, L. *Geoderma* **2014**, *s 232-234*, 600-608.